Opposing roles of FoxP1 and Nfat3 in transcriptional control of cardiomyocyte hypertrophy

Shoumei Bai and Tom K Kerppola*
Department of Biological Chemistry
University of Michigan
Ann Arbor, MI 48109-0650.

Supplemental material for:

Shoumei Bai and Tom K Kerppola. Opposing roles of FoxP1 and Nfat3 in transcriptional control of cardiomyocyte hypertrophy. Molecular and Cellular Biology 31 (14): 3068-3080. 2011.

URL: http://dx.doi.org/10.1128/MCB.00925-10
URL (Abstract): http://mcb.asm.org/cgi/content/abstract/31/14/3068
URL (Full Text): http://mcb.asm.org/cgi/content/full/31/14/3068
URL (PDF file): http://mcb.asm.org/cgi/reprint/31/14/3068.pdf

Table of Contents

* Corresponding author (kerppola@umich.edu). URL: http://sitemaker.umich.edu/kerppola

Supplemental Fig. S1

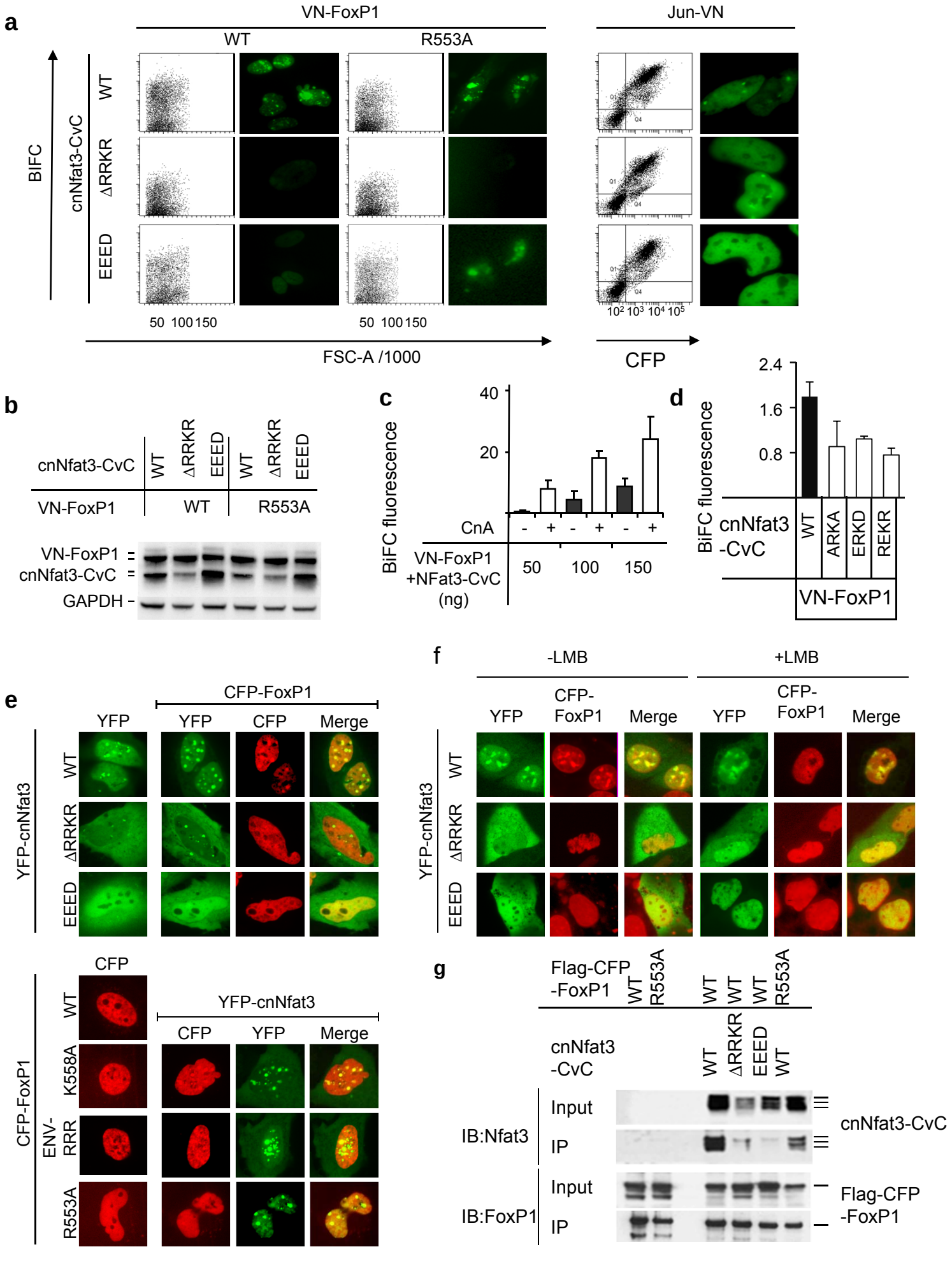

Supplemental Fig. S1. Specificity of cnNfat3-FoxP1 BiFC complexes.

a. Effects of mutations in FoxP1 and cnNfat3 on BiFC complex fluorescence

Procedure: HeLa cells were infected with lentiviruses encoding the combinations of cnNfat3 and FoxP1 or Jun fusion proteins indicated above and to the left of the images (WT: wild type, ΔRRKR: deletion and EEED: substitution of residues 672-675 in cnNfat3). The cells were imaged and their fluorescence intensities were measured by flow cytometry 2 days after infection. The scatter plots show the fluorescence intensities of individual cells (vertical axis) as a function of forward scatter (horizontal axis). The Jun fusions were co-transfected together with Fos-CFP, and the BiFC fluorescence intensities (vertical axis) were plotted as a function of CFP fluorescence (horizontal axis). The images are representative of the majority of cells in each population and the scatter plots are representative of three separate infections.

Results: Mutations at the interface between FoxP1 and cnNfat3 reduced the efficiency of FoxP1-cnNfat3 BiFC complex formation, but had a smaller effect on Jun-cnNfat3 BiFC complex formation. These results corroborate the specificities of the effects of the mutations in cnNfat3 on interactions with cnNfat3. FoxP1-cnNFat3 BiFC complexes formed nuclear foci in Hela cells. These foci were eliminated when the RRKR motif in Nfat3 was either deleted or substituted by EEED. FoxP1^{R553A}–cnNfat3 BiFC complexes were localized to large nuclear bodies. Jun-cnNfat3 BiFC complexes were uniformly distributed in the nucleoplasm with a small number of subnuclear foci.

b. Comparison of the levels of fusion protein expression.

Procedure: The levels of fusion protein expression in HeLa cells infected with lentiviruses encoding the proteins indicated above the lanes were measured by immunoblotting using antibodies directed against GFP. The data shown are representative of three separate infections.

Result: The mutations in cnNfat3 and FoxP1, and co-expression of the fusion proteins, had no detectable effect on their expression levels.

c. Effects of CnA expression on FoxP1-Nfat3 BiFC compex formation in HEK293T cells.

Procedure: The amounts (ng) of plasmids encoding FoxP1 and Nfat3 fusion proteins indicated below the bars were co-transfected into HEK293T cells together with (+) or without (-) a plasmid encoding the catalytic subunit of calcineurin (CnA – 500ng). The fluorescence intensities of the cells were measured by flow cytometry one day after transfection.

Result: CnA expression induced FoxP1-Nfat3 BiFC complex formation when limiting amounts of FoxP1 and Nfat3 were expressed. At higher levels of FoxP1 and Nfat3 expression, CnA enhanced the efficiency of BiFC complex formation. Two-factor ANOVA of the data from all experiments indicated that CnA expression had significant ($p<0.01$) effects on FoxP1-Nfat3 BiFC complex formation under each of the conditions examined.

d. Effects of amino acid substitutions in the RRKR motif of cnNfat3 on BiFC complex formation with FoxP1.

Procedure: Hela cells were transfected with plasmids encoding cnNfat3 containing the amino acid substitutions indicated below the bars and FoxP1 fusion proteins. Fluorescence intensities were measured 16 h after transfection by flow cytometry.

Result: Substitution of individual amino acid residues in the RRKR motif of cnNfat3 reduced BiFC complex formation with FoxP1. The data shown are representative of three or more independent experiments.

e. Effects of wild type or mutated cnNfat3 co-expression on FoxP1 subnuclear localization.

Procedure: The proteins indicated to the left and above the images were co-expressed in Hela cells. YFP (green) and CFP (red) fluorescence were imaged 16 hours after transfection (ENV-RRR: substitution of residues 555-557 in FoxP1 by RRR).

Result: FoxP1 was recruited to sub-nuclear foci by cnNfat3 co-expression, but not by cnNfat3$^{\Delta RRKR}$ or cnNfat3^{EEED} co-expression. cnNfat3$^{\Delta RRKR}$ and cnNfat3^{EEED} were localized to nuclei less efficiently than cnNfat3.

f. Effects of Leptomycin B (LMB) on cnNfat3 localization and on the subnuclear distribution of FoxP1.

Procedure: Hela cells were transfected with plasmids encoding the fusion proteins indicated to the left and above the images. The cells were treated with 10ng/ml LMB at 16 hours after transfection and were imaged 1 hour after LMB treatment.

Result: The efficiencies of nuclear localization varied among individual cells. LMB treatment enhanced the overall efficiencies of cnNfat3$^{\Delta RRKR}$ and cnNfat3^{EEED} nuclear localization. FoxP1 was not recruited to the nuclear foci formed by cnNfat3$^{\Delta RRKR}$ in LMB treated cells.

g. Effects of mutations in cnNfat3 on co-immunoprecipitation with FoxP1

Procedure: Plasmids encoding the FoxP1 and cnNfat3 fusion proteins indicated above each lane were co-transfected into HEK293T cells. The cells were lysed 24 hours after transfection, and the cell extracts were precipitated using anti-FLAG antibody. The immunoprecipitates were extensively washed and analyzed by immunoblotting using antibodies directed against FoxP1 and Nfat3. The input lanes contained 2% of the cell extract.

Result: cnNfat co-precipitated with FoxP1, and the amounts of cnNfat3$^{\Delta RRKR}$ and cnNfat3^{EEED} co-precipitated with FoxP1 were markedly lower. The amount of cnNfat3 co-precipitated with FoxP1^{R553A} was lower than the amount co-precipitated with wild type FoxP1.

Supplemental Fig. S2

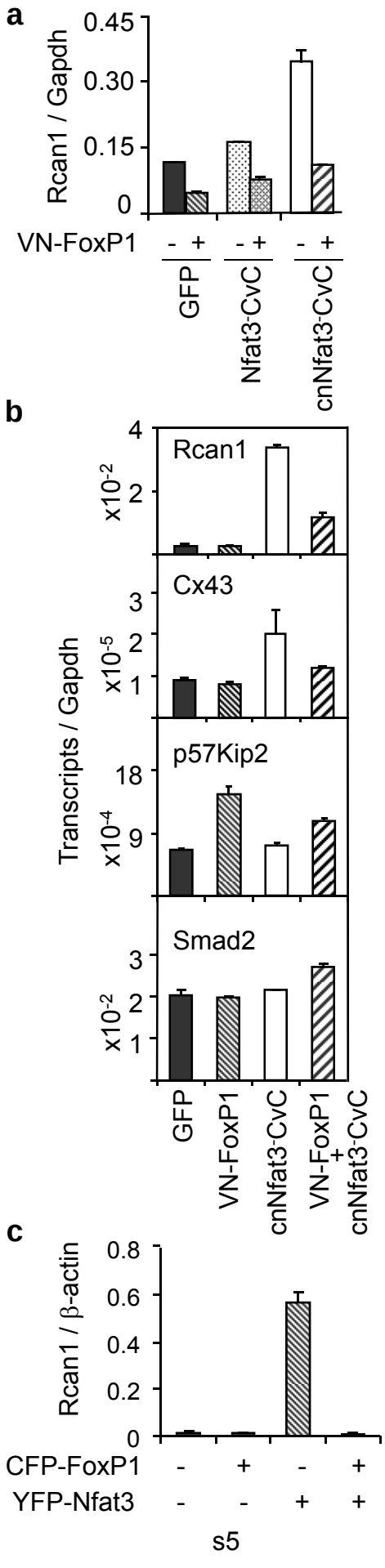

Supplemental Fig. S2. Effects of ectopic FoxP1, Nfat3 and cnNfat3 expression in neonatal cardiomyocytes and in H9C2 myoblasts on transcription of hypertrophy-associated genes.

a. Effects of ectopic FoxP1 and truncated or full length Nfat3 expression in neonatal cardiomyocytes on Rcan1 transcription.

Procedure: Primary rat cardiomyocytes were infected with lentiviruses encoding the combinations of FoxP1, Nfat3 and cnNfat3 fusion proteins indicated below the graphs. The levels of Rcan1 transcripts were measured 4 days after infection and were normalized by the levels of Gapdh transcripts. The data shown are representative of three separate experiments.

Result: Full length Nfat3 expression had a modest effect on endogenous Rcan1 transcription in neonatal cardiomyocytes, possibly because full length Nfat3 was predominantly cytoplasmic in these cells. The increase in Rcan1 transcription induced by ectopic Nfat3 expression was reversed by co-expression of FoxP1.

b. Effects of ectopic FoxP1 and cnNfat3 expression in H9C2 myoblasts on hypertrophy-associated gene transcription.

Procedure: H9C2 cells were infected with lentiviruses encoding the FoxP1 and cnNFat3 fusion proteins indicated below the graphs. The levels of the transcripts indicated in each graph were measured 4 days after infection and were normalized by the levels of Gapdh transcripts. The data in each panel is representative of five separate experiments.

Result: Ectopic FoxP1 and cnNfat3 have opposing effects on transcription. cnNfat3 activated and FoxP1 repressed Rcan1 as well as Cx43 transcription in H9C2 myoblasts. Conversely, FoxP1 activated p57Kip2 transcription and cnNfat3 counteracted p57Kip2 activation by FoxP1. The opposing effects of FoxP1 and cnNfat3 on transcription of both growth-promoting and growth-modulatory genes in primary rat cardiomyocytes and in H9C2 myoblasts suggest that these transcription factors have opposing roles in the control of myocyte growth.

c. Effects of ectopic FoxP1 and full length Nfat3 expression in H9C2 myoblasts on Rcan1 transcription.

Procedure: H9C2 cells were infected with lentiviruses encoding the FoxP1 and Nfat3 fusion proteins indicated below the graph. The levels of Rcan1 transcripts were measured 4 days after infection and normalized by the levels of β-actin transcripts. The data are representative of three separate experiments.

Result: Expression of full length Nfat3 activated Rcan1 transcription in H9C2 cells. Rcan1 activation by Nfat3 was reversed by FoxP1 co-expression.

Supplemental Fig. S3

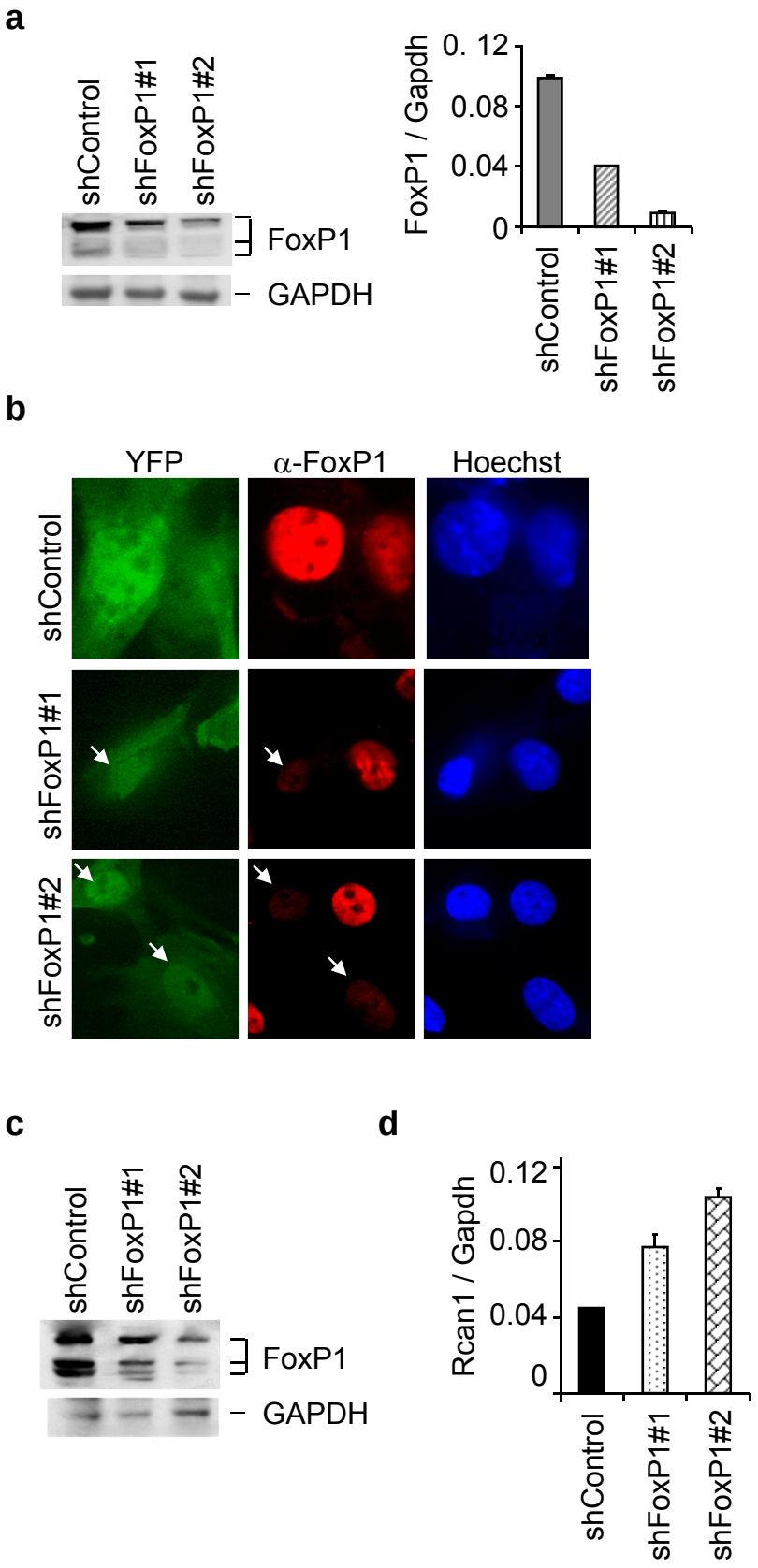

Supplemental Fig. S3. Efficiencies of FoxP1 knockdown in neonatal cardiomyocytes and H9C2 cells

a. Efficiency of FoxP1 knockdown in neonatal cardiomyocytes.

Procedure: The levels of FoxP1 transcripts and proteins were measured in primary rat cardiomyocytes infected with lentiviruses expressing the shRNA constructs indicated above the lanes and below the bars. The transcript and protein levels were measured four days after infection and the transcript levels were normalized by the levels of Gapdh transcripts.

Result: Infection of primary rat cardiomyocytes by lentiviruses expressing either of two different shRNAs directed against FoxP1 reduced the levels of endogenous FoxP1 transcripts by 50% and 80%, respectively. Similar decreases in the levels of endogenous FoxP1 proteins were observed. The data shown are representative of three separate experiments.

b. Efficiencies of FoxP1 knockdown in individual cardiomyocytes.

Procedure: The levels of FoxP1 protein expression (red) were measured by immunofluorescence four days after infection of primary rat cardiomyocytes with lentiviruses encoding the shRNAs indicated to the left of the images. GFP fluorescence (green) encoded by the lentiviruses and Hoechst staining of DNA (blue) were visualized in the same cells.

Result: FoxP1 protein levels were reduced in cardiomyocytes expressing FoxP1 shRNAs #1 or #2. The changes in the transcription of putative target genes caused by FoxP1 knock-down under-estimate the significance of FoxP1 in their regulation both because FoxP1 knockdown in the cardiomyocytes was not complete and because the small number of non-cardiomyocytes in the population was not efficiently infected by the lentiviral vectors. The images shown are representative of the variations in FoxP1 expression levels in each cell population.

c. Effects of FoxP1 knockdown in H9C2 myoblasts on Rcan1 transcription.

Procedure: H9C2 cells were infected by lentiviruses encoding the shRNA constructs indicated above the lanes and below the bars. Rcan1 transcripts were measured four days after infection and normalized by the levels of Gapdh transcripts. The levels of FoxP1 expression in the cells were measured by immunoblotting.

Result: FoxP1 knockdown derepressed Rcan1 transcription in H9C2 myoblasts. The data shown are representative of three separate experiments.

Supplemental Fig. S4

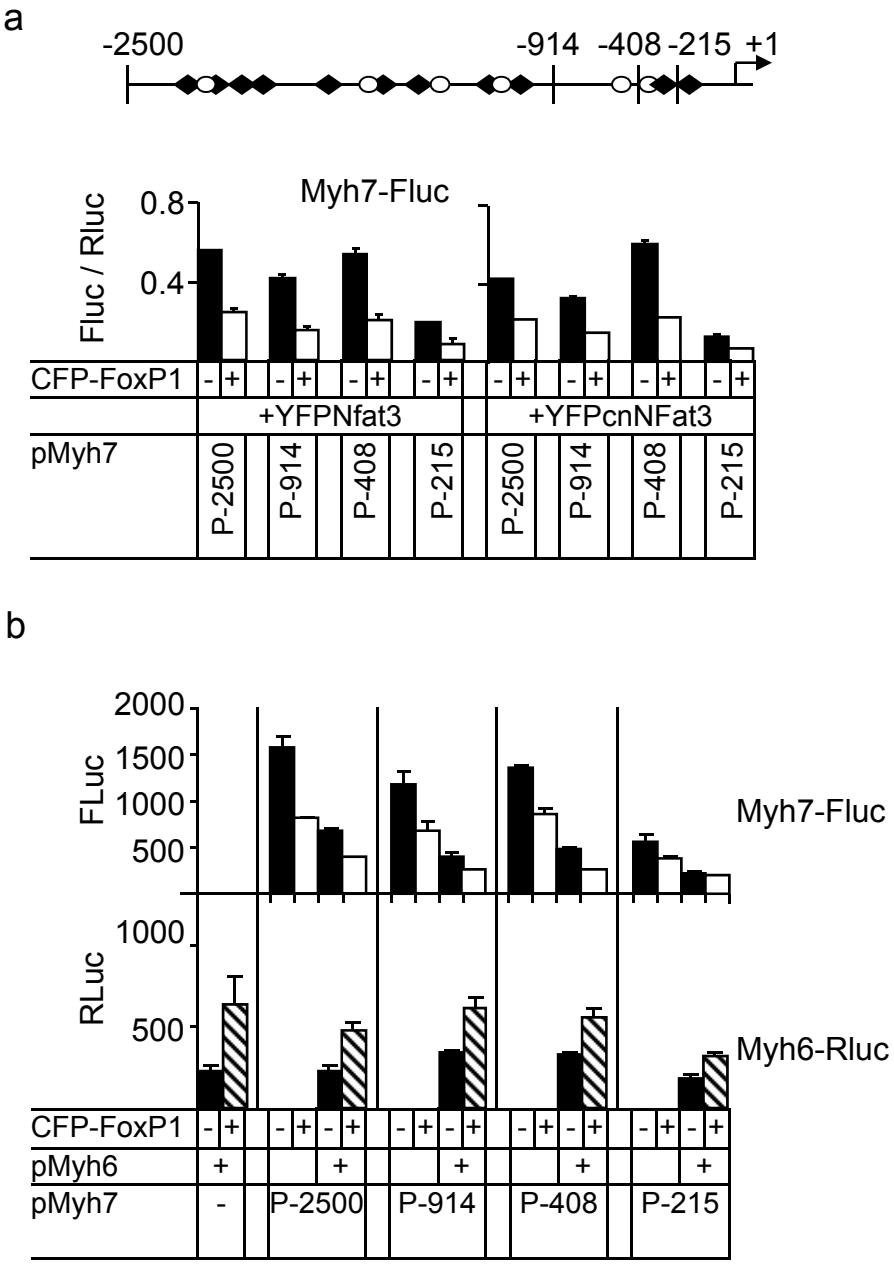

Supplemental Fig. S4. Regions of the Myh7 promoter required for Nfat3 activation and FoxP1 repression of reporter gene transcription.

a. Effects of truncations of the Myh7 promoter on Nfat3 activation and FoxP1 repression of reporter gene transcription in H9C2 cells

Procedure: Plasmids encoding FoxP1 and Nfat3 or cnNfat3 as indicated below the bars were co-transfected into H9C2 myocytes with reporter plasmids containing Myh7 promoter sequences controlling firefly luciferase (Fluc). An internal control plasmid encoding Renilla luciferace (Rluc) was included. The dual luciferase reporter activities were measured 20-22 hours after transfection. The diagram above the graph represents the Myh7 promoter region. FoxP recognition sequences are indicated by solid diamonds and Nfat recognition sequences are indicated by open circles. The numbers above the line indicate the positions where the promoter was truncated.

Result: The region between 215 and 408 base pairs upstream of the Myh7 transcription start site increased reporter gene activity. FoxP1 repressed all Myh7 reporter genes containing FoxP recognition sequences. The data shown are representative of three separate experiments. Two-factor ANOVA indicated that FoxP1 and Nfat3 individually had moderately significant ($p<0.05$) effects on expression of all of the Myh7 reporter genes tested. FoxP1 in combination with Nfat3 had effects that were significantly ($p<0.01$) different from those of the individual effects of FoxP1 and Nfat3.

b. Effect of FoxP1 on Myh7 and Myh6 promoter activities

Procedure: Plasmids encoding FoxP1 as indicated below the bars were co-transfected with Myh7 reporter constructs controlling firefly luciferase (Fluc), and a Myh6 reporter construct controlling Renilla luciferace (Rluc) separately or in combination into H9C2 cells. The dual luciferase reporter activities were measured 20-22 hours after transfection.

Result: FoxP1 had opposite effects on transcription of Myh7 and Myh6 reporter constructs in the same cells. The data shown are representative of six separate experiments for the Myh7(P-914) promoter. Two-factor ANOVA indicated that FoxP1 had significant ($p<0.01$) and opposite effects on both Myh7(P-914) and Myh6 reporter gene expression in the same cells.

Supplemental Fig. S5

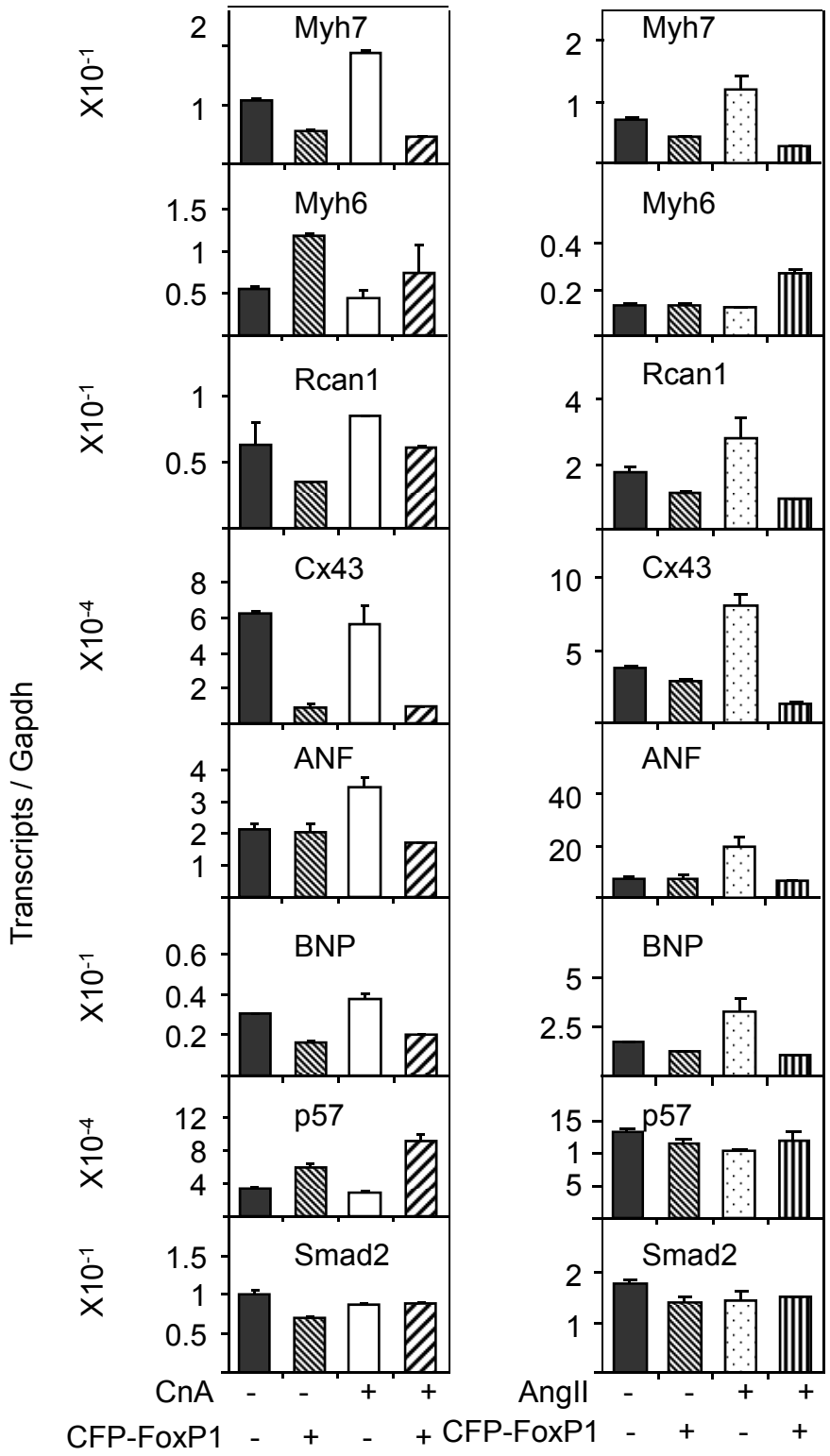

Supplemental Fig. S5. FoxP1 expression counteracts calcineurin and angiotensin II activation of hypertrophy-associated gene expression in cardiomyocytes.
Procedure: Neonatal cardiomyocytes were co-infected with lentiviruses encoding FoxP1 or CnA separately or in combination as inficated below the graphs (left column). Alternatively, neonatal cardiomyocytes were treated overnight with 10 nM angiotensin II (AngII), and were infected with lentivirus encoding FoxP1 as indicated below the graphs (right column). Angiotensin II treatment was resumed 24 hours after infection. The levels of the transcripts indicated in each graph were measured 4 days after infection and were normalized by the levels of Gapdh transcripts.
Result: FoxP1 expression counteracted hypertrophy-associated gene transcription stimulated by CnA expression or angiotensin II treatment of neonatal cardiomyocytes. The data in each graph are representative of two separate experiments.

Supplemental Fig. S6

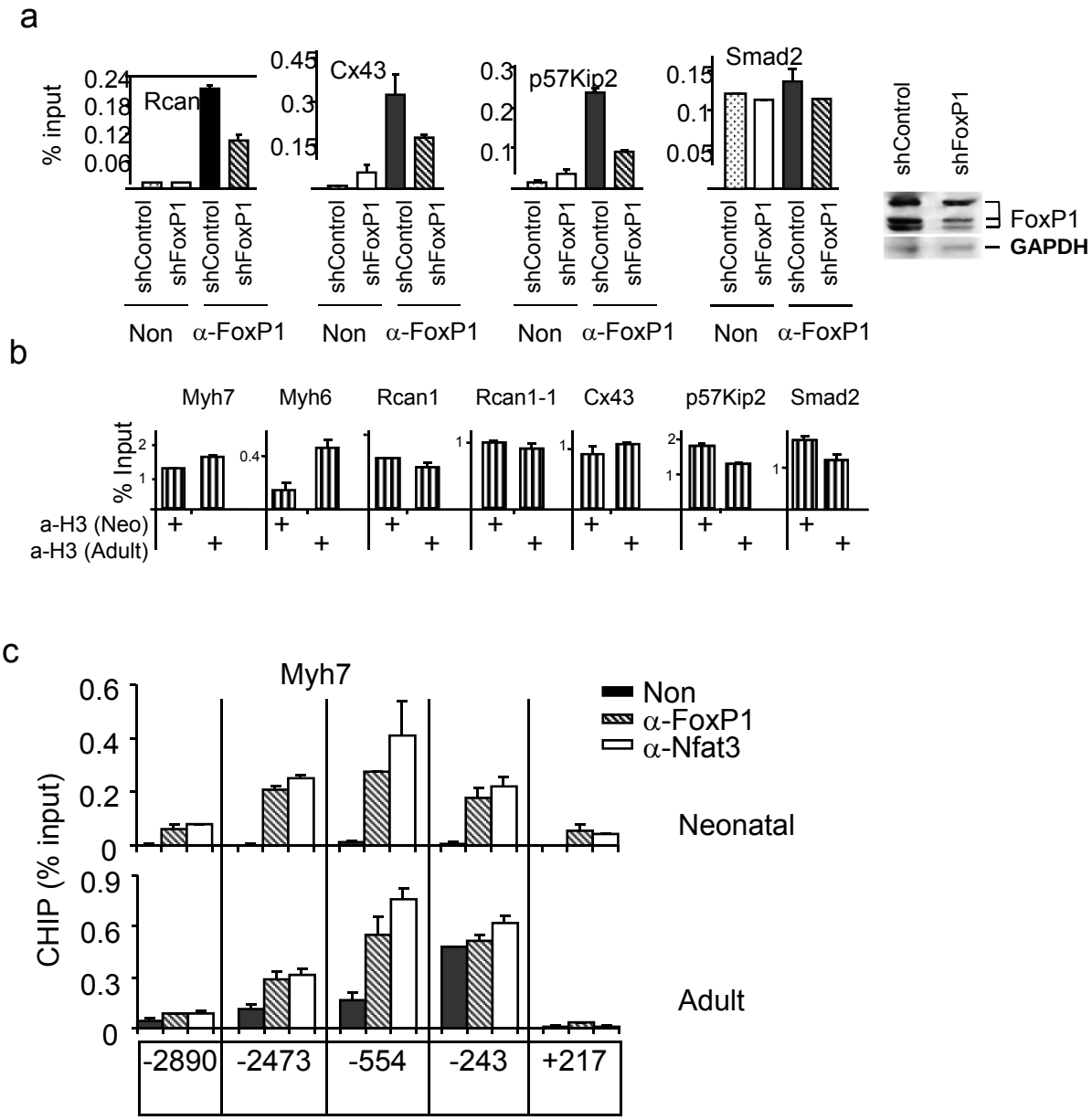

Supplemental Fig. S6. ChIP analysis of the effects of FoxP1 knockdown on promoter occupancy and regions of the Myh7 promoter occupied by FoxP1 and Nfat3

a. Effects of FoxP1 knockdown on promoter occupancy in H9C2 myoblasts.

Procedure: H9C2 myoblasts were infected with lentiviruses encoding the shRNAs indicated below the graphs. 4 days after infection, chromatin isolated from the cells was precipitated using antibodies directed against FoxP1 or using non-immune serum (Non). The chromatin was analyzed by qPCR using primers designed to amplify the promoter region indicated in each graph (Table S1).

Result: FoxP1 occupancy at the Rcan1, Cx43 and p57Kip2 promoters was reduced when FoxP1 was depleted by shRNA knockdown in H9C2 Cells. The data shown are representative of three separate experiments.

b. Histone H3 occupancy at hypertrophy-associated promoters in neonatal and adult hearts.

Procedure: Chromatin isolated from neonatal or adult rat hearts was precipitated using antibody directed against H3 as shown below the bars. The precipitates were analyzed by qPCR using primers designed to amplify genes as shown on the top of the graphs

Result: The efficiency of promoter occupancy by H3 was similar in neonatal and adult hearts. The difference observed at the Myh6 promoter was not observed in other experiments.

c. Regions of the Myh7 promoter occupied by FoxP1 and Nfat3 in rat heart.

Procedure: Chromatin isolated from neonatal (upper panel) or adult (lower panel) rat hearts was precipitated using antibodies directed against FoxP1 or Nfat3 or Non-immune serum (Non) as shown below the bars. The precipitates were analyzed by qPCR using primers designed to amplify the Myh7 promoter. The numbers below the graphs represent the midpoints of the fragments (<140bp) amplified by qPCR.

Result: FoxP1 and Nfat3 occupied the same region of the Myh7 promoter from about 200 to 2000 bp upstream of the transcription start site in both neonatal and adult heart. The data shown are representative of three separate experiments.

Supplemental Fig. S7

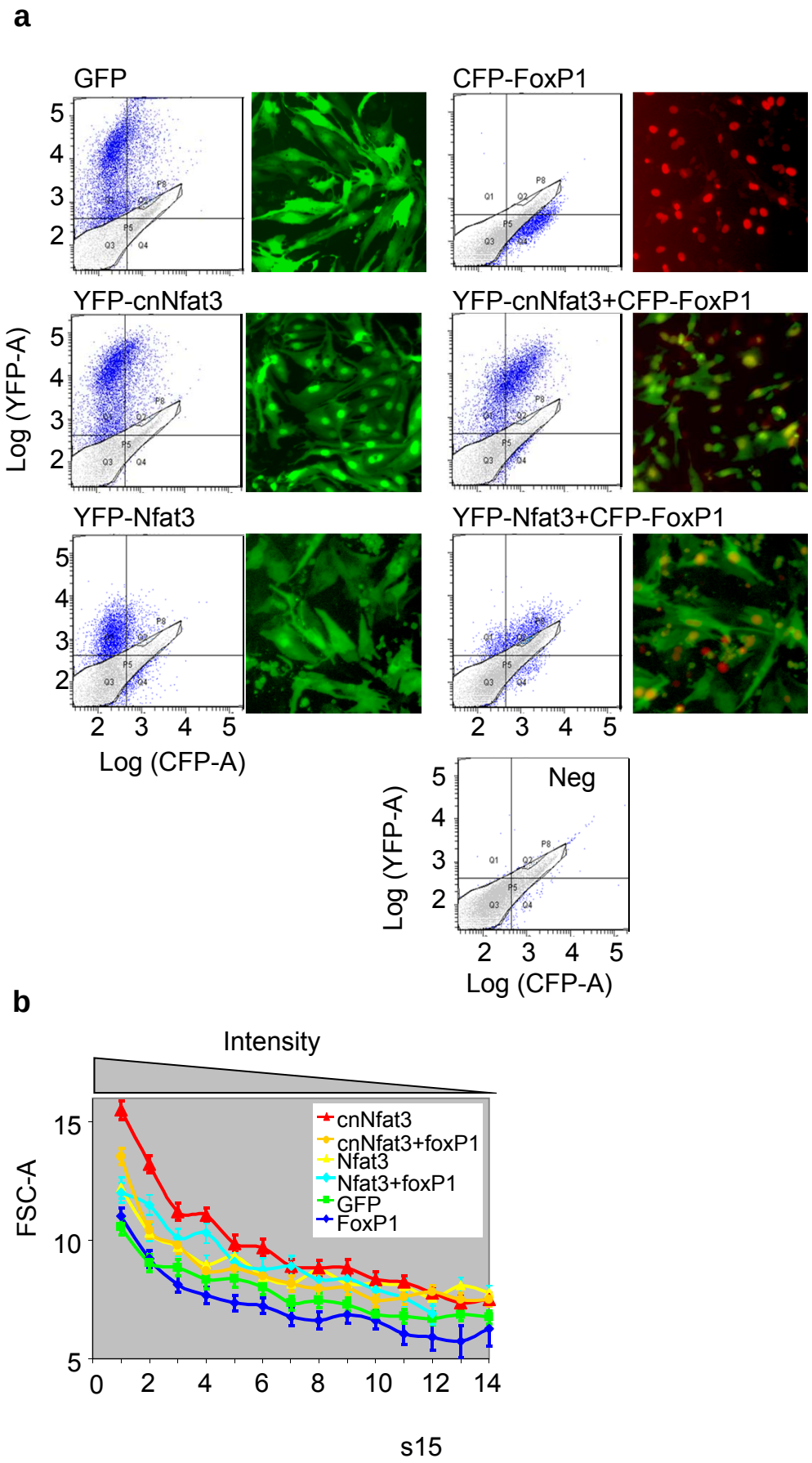

Supplemental Fig. S7. Effects of ectopic FoxP1 and Nfat3 expression on cardiomyocyte growth.

a. Fluorescence images and intensities of cardiomyocytes used for analysis of cell size by flow cytometry (YFP/GFP - green, CFP – red).

Procedure: Cardiomyocytes were imaged 4 days after infection with lentiviruses expressing the fusions indicate above the plots. The fluorescence intensities and forward scatter (shown in part b) were measured by flow cytometry. The YFP (or GFP) and CFP intensities were plotted as a scatter plots. Uninfected cells (Neg) were analyzed in parallel and were used to gate out the uninfected subpopulation (outlined and plotted in grey).

Result: Lentiviral infection produced detectable fusion protein expression in more than 80% of cardiomyocytes. Likewise, more than 80% of the cells were cardiomyocytes identified based on anti-α-actinin staining. The cells with no fluorescence (grey) were gated out from the population (blue) whose forward and side scatter intensities (not shown) were measured. The data shown are representative of three separate experiments.

b. Effects of differences in the levels of YFP-cnNfat3, YFP-Nfat3 and CFP-FoxP1 expression on cardiomyocyte size.

Procedure: Cardiomyocytes expressing different combinations of YFP-cnNfat3, YFP-Nfat3 and CFP-FoxP1 (shown in a) were binned in groups of 200 cells based on fluorescence intensity. The median forward scatter (FSC-A) for each group was calculated and plotted in order of decreasing fluorescence intensity. The error bars represent the coefficient of variation of the forward scatter values within each group.

Result: Cardiomyocytes that expressed the highest levels of ectopic cnNfat3 and Nfat3 had the highest forward scatter. Co-expression of FoxP1 reduced the mean forward scatter of cells that expressed either cnNfat3 or Nfat3. The data shown are representative of three separate experiments.

Supplemental Methods

Plasmids. FoxP1 and variants thereof were fused to the N-terminal 172 amino acid residues of Venus (VN) or to CFP at their N-termini. Nfat3 and cnNfat3 (lacking the N-terminal 317 amino acid residues of Nfat3) and mutants thereof were fused to residues 173-238 of Cerulean with the S177G substitution (CvC) at their C-termini or to YFP at their N-termini. FoxP1 (accession # BC064764.1) and Nfat3 (accession# BC028928) image clones were obtained from ATCC. To generate the plasmid encoding VN-FoxP1, the coding sequence of FoxP1 was inserted between the Xba1 and BamH1 sites in plasmid pVN173CBX2 (12). To generate plasmids encoding Nfat3-YC and cnNFat3-YC, the coding sequences of Nfat3 or cnNFat3 were first inserted between the Sal1 and BamH1 sites of pH3.2Venus (12). Subsequently, the sequence encoding Venus was replaced with the sequence encoding CvC (16). The Jun-VN expression vector was provided by Dr. Chang-Deng Hu (Purdue University) and has been described (6). The CFP-Fos expression vector was constructed by Dr. Yurii Chinenov and was made by fusing the sequence encoding CFP to the N-terminal end of Fos.
To prepare lentiviral expression vectors, the sequences encoding FoxP1, Nfat3 and cnNfat3 fusion proteins were subcloned into the pGIPZ lentiviral vector (Open Biosystems, Thermo Fisher, Huntsville, AL). cnNfat3$^{\Delta RRKR}$ and Nfat3$^{\Delta RRKR}$ correspond to cnNfat3 and Nfat3 in which residues 672-675 were deleted. cnNfat3^{EEED} and Nfat3^{EEED} corresponds to cnNfat3 and Nfat3 in which residues 672-675 were substituted by EEED. FoxP1^{R553A} corresponds to FoxP1 in which residue 553 was substituted by alanine.

Culture of neonatal rat cardiomyocytes. Cardiomyocytes were isolated from 1-3 day old Sprague Dawley rats by enzymatic digestion of miced hearts with type II collagenase (Worthington) and pancreatin (Sigma) (2). The dissociated cardiomyocytes were cultured in D-MEM/Ham F12 (1:1) supplemented with 10% FBS, 5% horse serum, 0.2% BSA (Fraction V), 4μg/ml transferrin, 0.7 ng/ml sodium selenite and 5μg/ml linoleic acid (23). Twenty-four hours later the medium was replaced with medium lacking FBS and horse serum.

Microscopy and flow cytometry analysis. BiFC complexes as well as YFP and CFP fusion proteins were visualized in live cardiomyocytes, Hela and HEK393T cells. For simultaneous immunofluorescence imaging, cardiomyocytes were fixed in 2% paraformaldehyde. The fixed cells were incubated with anti-FoxP1 (rabbit, a gift from E. Morrisey, University of Pennsylvania) (17) , anti-GFP (rabbit, Fitzgerald), anti-actinin (mouse, sigma), or anti connexin-43 (mouse, sigma) antibodies where indicated. The immune complexes were detected using alexa647-anti-mouse, FITC-anti-rabbit, or alexa647-anti-rabbit secondary antibodies (Invitrogen). Images were captured using an Olympus IX81 DSU microscope with a Hamamatsu ORCA-ER CCD camera. YFP fluorescence was excited at 500/20 nm and emission was collected at 535/30 nm. CFP fluorescence was excited at 436/10 nm and emission was collected at 470/30 nm.
BiFC fluorescence was quantified in Hela cells by flow cytometry analysis 2-4 days after lentiviral infection or 16 hours after transfection. FITC, DAPI and APE filters were used to detect cells expressing YFP (GFP or BiFC), CFP and alexa 647 staining, respectively. Flow cytometry data was analyzed using Flowjo and Becton Dickinson FACS Diva software.

Isolations of chromatin for ChIP analysis. Neonatal and adult rat hearts were excised, minced and washed quickly in cold PBS. The tissue was cross-linked in 1.5% paraformaldehyde for 30 minutes. The cross-linked tissue was disaggregated by dounce homogenization in cold PBS containing a cocktail of protease inhibitors (Roche) and PMSF (1mM). The cells were lysed by dounce homogenization in 50 mM Hepes pH 7.9, 140 mM NaCl, 1 mM EDTA, 0.25% Triton X-100, 0.5% NP-40, 0.5 mM PMSF, and protease inhibitors. The nuclei were pelleted by centrifugation at 500g for 5 min. The nuclei were washed in 10 mM Tris-HCl pH 8.0, 1 mM

EDTA, 150 mM LiCl and lysed in 0.05% SDS, 1% Triton X-100, 2 mM EDTA, 20 mM Tris-HCl, pH 8.1, 150 mM NaCl. The chromatin was sheared using a Bioruptor (Diagenode) and the solubilized chromatin was precipitated using the antibodies indicated. Chromatin isolated from the equivalent of one neonatal heart was incubated with each antibody. The amount of chromatin isolated from adult hearts was adjusted to be the same as that isolated from one neonatal heart by measurement of the DNA concentration. ChIP was performed as described (1).
When H9C2 cells were used for ChIP analysis, the cells were cross-linked in 1.5% paraformaldehyde for 15min. Isolation on nuclei and chromatin preparation were performed as described above for the heart tissue.

Sequential ChIP analysis. The ChIP procedure was as described (25) with the following modification. Two hearts from 15-16 day rats were used for 1st ChIP per antibody or non-immune sera. The chromatin from the 1st ChIP was eluted with 50mM $NaCO_3$, 0.5% SDS at 37^{o}C. 90% of the eluate was diluted in the immunoprecipitation buffer and the chromatin was re-immunoprecipitated using the same ChIP procedure (25). 10% of the eluate from the 1st ChIP was analyzed in parallel with the total eluate from the 2nd ChIP.

shRNA knockdown and analysis. Plasmids encoding shRNAs targeting FoxP1 and control shRNA were obtained from Open Biosystems. Cardiomyocytes and H9C2 cells were infected with shRNA packaged in lentiviral particles. The cells were harvested 2-4 days after infection and subjected to analysis. FoxP1 levels were monitored by immunoblotting and immunofluorescence analysis using anti-FoxP1 antibodies.

Transcript quantitation. RNA was isolated using the RNAeasy mini Kit (Qiagen). cDNA was synthesized using the Reverse Transcriptase System (Promega). Transcripts were quantified by qPCR using the primers listed in Supplemental Table S1 and SYBR green I master mix (Roche) with a LightCycler480 II (Roche) instrument. The transcript levels were quantified by assuming that transcript abundance was proportional to $2^{-\Delta ct}$ (ct: threshold cycle number).

Reporter gene assays. H9C2 myoblast and Hela cells were transfected using Fugene 6. Plasmids encoding the FoxP1, Nfat3 and cnNfat3 fusion proteins indicated were co-tranfected with reporter plasmids containing the Rcan1, Myh6 or Myh7 promoters and internal control plasmids (19, 24). In some experiments, the cells were treated with ionomycin (2□M) for five hours with or without cyclosporine A (CsA, 10□M) pretreatment for twenty minutes. The luciferase activities were measured 20-22 hours after transfection in cells extracts using a dual luciferase assay kit (Promega).

Supplemental Table S1. Sequences of oligonucleotides used for transcript quantitation

Myh7	F:GAGGAGAGGGCGGACATT R:ACTCTTCATTCAGGCCCTTG
Myh6	F:TGCAGAAGAAACTGAAGGAAAA F:GCTCGGCCTCTAGCTCCT
Rcan1	Rat: F:TAAGCGTCTGCCCGTTGAAAAAGC R:GGATTCAAATTTGGCCCTGGTCTC
	Human: F:TAGCTCCCTGATTGCCTGTGTGG R:GCGGAGAAGGGGTTGCTGAAGT
Cx43	F:AGCCTGAACTCTCATTTTTCCTT R:CCATGTCTGGGCACCTCT
Anf	F:TCCGGTACCGAAGATAACAG R:TCGTGATAGATGAAGACAGGAAG
Bnp	rBnp-RTF:TGATTCTGCTCCTGCTTTTCCTTA rBnp-RTR:AGCCATTTCCTCTGACTTTTCTCT
p57Kip2	F:GTCCATCACCAATCAGCCAGCA R:CTCGCGGCCCAGCTCCTC
Smad2	F:CATGCGTCACAGCCCTCACTCA R:CACTCCCCTTCCTATATGCCTTCTG
GAPDH	F:GGCCGGTGCTGAGTATGTCGTG R:TCGGCAGAAGGGGCGGAGAT
β-actin	F:CACTCTTCCAGCCTTCCTTCC R:CTCAGGAGGAGCAATGATCTTG

Supplemental Table S2. Sequences of oligonucleotides used in ChIP analysis

Myh7	+217bp F:AACACTCCCCTGCAGGTCTAAATA R:ACACGCACACGCACACGCA -243bp F:CTTGAGGTCATGGTGGTCGTGGTC R:TTGGAAGTGGGCGTCATTGTTGTG -554bp F:CTGAGCCGGAGTTCCTGTGTCTGA R:GGTATGGCCCTGGTATGGTGGTTG -2473bp F:GAGCCCAGACAAAGCAGACACAAT R:TTCGCTGAGGTAGACCAAATAAGG -2890bp F:AGCAGCCGGAATACAAAAGAACGA R:CCTAGCTGCCTGAATCCCTGACCT
Myh6	F:TTCTCCTTTTCCACGTGTTTCTCA R:GTGTATGAAGCCCTGGGTTTGATT
Ran1	-200bp F: CGGAGCAGAGGTAATTAGCATAGG: R: CTCAGGCAGACAGGGACAAAGTG: -800bp F: GCCCCACAGCTACAGTAAGGAAGT R: GTTTGTTTTGAAGTCAGCGTTTTT -2700bp F: TGGGGAACAAAGGGACTGAC R: GCTGCTGCCTGTGGGACTCT
Rcan1-1	F: GGTTGGGGCATTTTATCACAGTA R: GCCCTTTCTCCAATCCTGCTGAC
Cx43	F: ATCACGCACACCCACCTCAA R: CACTGCAGGGCTGTGACTCCTC
P57Kip2	F: GAGTATCCAGGGCCCCACCAAGAG R: GCCATATTCCGCCCCCAGTTC
Smad2	F: GCCGCCCGAAGGTAGGT R: GAGCCGCCTGCTCCACTC

References

1. **Bai, S., K. Ghoshal, and S. T. Jacob.** 2006. Identification of T-cadherin as a novel target of DNA methyltransferase 3B and its role in the suppression of nerve growth factor-mediated neurite outgrowth in PC12 cells. J Biol Chem **281:**13604-11.
2. **Birla, R. K., Y. C. Huang, and R. G. Dennis.** 2007. Development of a novel bioreactor for the mechanical loading of tissue-engineered heart muscle. Tissue Eng **13:**2239-48.
3. **Davies, K. J., G. Ermak, B. A. Rothermel, M. Pritchard, J. Heitman, J. Ahnn, F. Henrique-Silva, D. Crawford, S. Canaider, P. Strippoli, P. Carinci, K. T. Min, D. S. Fox, K. W. Cunningham, R. Bassel-Duby, E. N. Olson, Z. Zhang, R. S. Williams, H. P. Gerber, M. Perez-Riba, H. Seo, X. Cao, C. B. Klee, J. M. Redondo, L. J. Maltais, E. A. Bruford, S. Povey, J. D. Molkentin, F. D. McKeon, E. J. Duh, G. R. Crabtree, M. S. Cyert, S. de la Luna, and X. Estivill.** 2007. Renaming the DSCR1/Adapt78 gene family as RCAN: regulators of calcineurin. FASEB J **21:**3023-8.
4. **Genesca, L., A. Aubareda, J. J. Fuentes, X. Estivill, S. De La Luna, and M. Perez-Riba.** 2003. Phosphorylation of calcipressin 1 increases its ability to inhibit calcineurin and decreases calcipressin half-life. Biochem J **374:**567-75.
5. **Kingsbury, T. J., and K. W. Cunningham.** 2000. A conserved family of calcineurin regulators. Genes Dev **14:**1595-604.
6. **Liu, H., X. Deng, Y. J. Shyu, J. J. Li, E. J. Taparowsky, and C. D. Hu.** 2006. Mutual regulation of c-Jun and ATF2 by transcriptional activation and subcellular localization. EMBO J **25:**1058-69.
7. **Liu, Z. P., Z. Wang, H. Yanagisawa, and E. N. Olson.** 2005. Phenotypic modulation of smooth muscle cells through interaction of Foxo4 and myocardin. Dev Cell **9:**261-70.
8. **McKinsey, T. A., and E. N. Olson.** 2005. Toward transcriptional therapies for the failing heart: chemical screens to modulate genes. Journal of Clinical Investigation **115:**538-46.
9. **Ni, Y. G., N. Wang, D. J. Cao, N. Sachan, D. J. Morris, R. D. Gerard, O. M. Kuro, B. A. Rothermel, and J. A. Hill.** 2007. FoxO transcription factors activate Akt and attenuate insulin signaling in heart by inhibiting protein phosphatases. Proc Natl Acad Sci U S A **104:**20517-22.
10. **Rajabi, M., C. Kassiotis, P. Razeghi, and H. Taegtmeyer.** 2007. Return to the fetal gene program protects the stressed heart: a strong hypothesis. Heart Fail Rev **12:**331-43.
11. **Razeghi, P., M. E. Young, J. L. Alcorn, C. S. Moravec, O. H. Frazier, and H. Taegtmeyer.** 2001. Metabolic gene expression in fetal and failing human heart. Circulation **104:**2923-31.
12. **Ren, X., C. Vincenz, and T. K. Kerppola.** 2008. Changes in the distributions and dynamics of polycomb repressive complexes during embryonic stem cell differentiation. Mol Cell Biol **28:**2884-95.
13. **Ronnebaum, S. M., and C. Patterson.** 2010. The FoxO family in cardiac function and dysfunction. Annu Rev Physiol **72:**81-94.
14. **Sanna, B., E. B. Brandt, R. A. Kaiser, P. Pfluger, S. A. Witt, T. R. Kimball, E. van Rooij, L. J. De Windt, M. E. Rothenberg, M. H. Tschop, S. C. Benoit, and J. D. Molkentin.** 2006. Modulatory calcineurin-interacting proteins 1 and 2 function as calcineurin facilitators in vivo. Proc Natl Acad Sci U S A **103:**7327-32.
15. **van der Vos, K. E., and P. J. Coffer.** 2008. FOXO-binding partners: it takes two to tango. Oncogene **27:**2289-99.

16. **Vincenz, C., and T. K. Kerppola.** 2008. Different polycomb group CBX family proteins associate with distinct regions of chromatin using nonhomologous protein sequences. Proc Natl Acad Sci U S A **105:**16572-7.

17. **Wang, B., J. Weidenfeld, M. M. Lu, S. Maika, W. A. Kuziel, E. E. Morrisey, and P. W. Tucker.** 2004. Foxp1 regulates cardiac outflow tract, endocardial cushion morphogenesis and myocyte proliferation and maturation. Development **131:**4477-87.

18. **Liu, H., X. Deng, Y. J. Shyu, J. J. Li, E. J. Taparowsky, and C. D. Hu.** 2006. Mutual regulation of c-Jun and ATF2 by transcriptional activation and subcellular localization. EMBO J **25:**1058-69.

19. **Wright, C. E., P. W. Bodell, F. Haddad, A. X. Qin, and K. M. Baldwin.** 2001. In vivo regulation of the beta-myosin heavy chain gene in hypertensive rodent heart. Am J Physiol Cell Physiol **280:**C1262-76.

20. **Wright, S. E., K. A. Rewers-Felkins, I. S. Quinlin, W. E. Fogler, C. A. Phillips, M. Townsend, W. Robinson, and R. Philip.** 2008. MHC-unrestricted lysis of MUC1-expressing cells by human peripheral blood mononuclear cells. Immunol Invest **37:**215-25.

21. **Wu, Y., M. Borde, V. Heissmeyer, M. Feuerer, A. D. Lapan, J. C. Stroud, D. L. Bates, L. Guo, A. Han, S. F. Ziegler, D. Mathis, C. Benoist, L. Chen, and A. Rao.** 2006. FOXP3 controls regulatory T cell function through cooperation with NFAT. Cell **126:**375-87.

22. **Xia, Y., J. B. McMillin, A. Lewis, M. Moore, W. G. Zhu, R. S. Williams, and R. E. Kellems.** 2000. Electrical stimulation of neonatal cardiac myocytes activates the NFAT3 and GATA4 pathways and up-regulates the adenylosuccinate synthetase 1 gene. J Biol Chem **275:**1855-63.

23. **Yamamoto, S., K. Seta, C. Morisco, S. F. Vatner, and J. Sadoshima.** 2001. Chelerythrine rapidly induces apoptosis through generation of reactive oxygen species in cardiac myocytes. J Mol Cell Cardiol **33:**1829-48.

24. **Yang, J., B. Rothermel, R. B. Vega, N. Frey, T. A. McKinsey, E. N. Olson, R. Bassel-Duby, and R. S. Williams.** 2000. Independent signals control expression of the calcineurin inhibitory proteins MCIP1 and MCIP2 in striated muscles. Circ Res **87:**E61-8.

25. **Vastenhouw, N. L., Y. Zhang, I. G. Woods, F. Imam, A. Regev, X. S. Liu, J. Rinn, and A. F. Schier.** 2010. Chromatin signature of embryonic pluripotency is established during genome activation. Nature **464:**922-6.